X-Ray Cherenkov Radiation as a Source for Transverse Size Diagnostics of Ultra-relativistic Electron Beams

A S Konkov[1], P V Karataev[2], A P Potylitsyn[1] and A S Gogolev[1]

[1] Tomsk Polytechnic University, Lenin Ave. 30, Tomsk, 634050, Russian Federation
[2] John Adams Institute at Royal Holloway, University of London, Egham, Surrey, TW20 0EX, UK

E-mail: anatoliy.konkov@gmail.com

Abstract. Development of advanced non-invasive methods for charged particle beam diagnostics is crucial in modern and future accelerators. Therefore, it is essential to develop non-invasive methods to generate EM radiation which properties depend on the beam parameters. In this paper we propose to use X-ray Cherenkov radiation (XCR) which can be generated by ultrarelativistic charged particles in the vicinity of the absorption edges of several materials. Due to a resonant nature of the refractive index near the absorption edges the generated radiation is quasi-monochromatic. On the other hand its properties depend on the parameters of the incident particle beam. In this paper we represent an approach for calculating the XCR generated along with transition radiation and diffraction radiation. The effect of the transverse electron beam size on the XCR characteristics is discussed.

1. Introduction

Polarization radiation (PR) generated by relativistic charged particles has been intensively studied as a source for various applications. It appears as a result of dynamic polarization of a medium [1]. Easily detectable photon yield resulted in development of precise methods for transverse beam size diagnostics using optical transition radiation (OTR) [2]. Due to a very low energy loss of the particles such PR types as diffraction radiation (DR) [3] and Smith-Purcell radiation [4] give opportunities to develop non-invasive methods for charged particle beam diagnostics. If the radiation wavelength is longer than the bunch length the radiation is emitted coherently, i.e. the photon yield is proportional to the squared number of particles in the bunch [1], enabling scientists to use the PR mechanism as an intense source of THz radiation with known polarization and spectral-spatial characteristics [5].

Transverse beam size and emittance diagnostics are one of the most challenging tasks in modern and future accelerators such as electron-positron linear colliders [6] or X-ray free electron lasers [7]. OTR and optical DR (ODR) based methods are the most promising ones. However, they benefit from the fact that the radiation is incoherent, i.e. each electron emits radiation independently. However in the state-of-the-art X-ray FELs the bunch length is very short and the longitudinal structure is such that some small fraction of the beam might generate radiation coherently in optical wavelength range [8] excluding OTR/ODR phenomena from the list of

potential candidates for the beam size monitoring. Moreover, the diagnostics requirements are so strict that the resolution of the OTR/ODR techniques is limited by diffraction.

Keeping in mind that the transition radiation (TR)/DR spectra are very broad then one of the solutions is to use shorter wavelength of the generated radiation to reduce both the diffraction limit and the coherency effects. For example, the EUV TR monitor is being developed in Mainz (Germany) [9]. A similar approach was proposed for UV/X-DR monitor in Cornell electron synchrotron Test Accelerator (CesrTA, Cornell) [10]. However, the UV or even X-ray frequency is comparable to or shorter than the plasmon frequency of metals. It means that the photon yield is either significantly supressed or requires a very special generation and observation geometry. In [11] authors have proposed to use the parametric X-ray radiation for transverse beams size measurements. In this paper we propose to use X-ray Cherenkov radiation (XCR) as a promising source for extremely low emittance charged particle beam diagnostics.

Cherenkov radiation (CR) is generated when a charged particle moves in a medium with velocity larger than the phase velocity of light in that medium, i.e. $v > c/n$, where n is the real part of the refractive index. Since the refractive index is a function of wavelength and is reduced towards shorter wavelength, the CR in almost entire X-ray region is either significantly suppressed or absent because the real part of the refractive index is smaller than unity. However, in [12] the authors have realized that in the vicinity of the atomic absorption edges the refractive index at high frequencies experiences a resonant increase. In this case the CR can be generated in X-ray region. Moreover, due to the fact that the refractive index has a sharp peak in the dispersion curve, CR spectrum is quasi-monochromatic with the bandwidth defined by the dispersion resonance.

In [13] the XCR at the K-edge of carbon generated by 1 GeV electrons was observed experimentally. Later the XCR generated by moderately relativistic electrons in titanium and vanadium foils at 5 MeV [14] and in silicon foil at 10 MeV [15] and at 75 MeV [16] was measured and investigated.

In this paper we represent a theoretical approach for calculating the characteristics of the XCR along with transition/diffraction radiation generated from the target surface. We performed a detailed analysis of the spectral-spatial properties and their distortion due to the beam size effect.

2. Theoretical formalism

The theoretical approach is based on the method of *polarization currents* [17–20]. The field of the PR emitted by medium atoms excited (polarized) by the external field $\mathbf{E}^0$ of the passing particle with energy $\gamma = E/(mc^2) = 1/\sqrt{1-\beta^2}$ moving rectilinearly and with constant velocity $\mathbf{v} = \beta c$ in a substance (or in its vicinity) can be represented as a solution of *vacuum* macroscopic Maxwell equations. Here γ is the charged particle Lorentz-factor, c is the speed of light, and m is the mass of the particle. For a non-magnetic medium the density of the polarization currents in a right hand side of the equations can be written as

$$\mathbf{j}_{pol} = \sigma(\omega)\Big(\mathbf{E}^0 + \mathbf{E}^{pol}(\mathbf{j}_{pol})\Big), \tag{1}$$

where $\mathbf{E}^0 \equiv \mathbf{E}^0(\mathbf{r},\omega)$ and $\mathbf{E}^{pol} \equiv \mathbf{E}^{pol}(\mathbf{r},\omega)$ are the Fourier image of the particle filed in vacuum and the field generated by the currents induced in the medium. The medium conductivity $\sigma(\omega)$ is related to the dielectric permittivity $\varepsilon(\omega)$ as

$$\sigma(\omega) = \frac{i\omega}{4\pi}(1-\varepsilon(\omega)), \tag{2}$$

here $\omega = 2\pi c/\lambda$, with λ being the radiation wavelength. Solving the Maxwell equations in a wave-zone for a target of finite volume V_T one can derive an expression for magnetic field $\mathbf{H}^{pol}$

of the PR emitted by the medium atoms excited by the passing particle filed in the form

$$\mathbf{H}^{pol}(\mathbf{r},\omega)=\nabla\times\frac{1}{c}\int_{V_T}\sigma(\omega)\mathbf{E}^0(\mathbf{r}',\omega)\frac{\exp\left(i\sqrt{\varepsilon(\omega)}|\mathbf{r}'-\mathbf{r}|\omega/c\right)}{|\mathbf{r}'-\mathbf{r}|}d^3r'. \tag{3}$$

In this model we assume that the energy loss by the particle is negligibly small in comparison to its total energy. One should note that (3) is an exact solution of Maxwell equations which allows us to avoid solving the differential equation (1). When we took into account the second term in (1), the wave number ω/c in vacuum was simply replaced by $\sqrt{\varepsilon(\omega)}\omega/c$. Such replacement describes the *renormalization* of the particle field inside the medium due to the field of the polarization currents [18,21]. Despite of a simple form equation (3) describes all types of PR generated in a medium of an arbitrary conductivity and an arbitrary inhomogeneity (i.e. in a target of an arbitrary shape), which is the main advantage of the method.

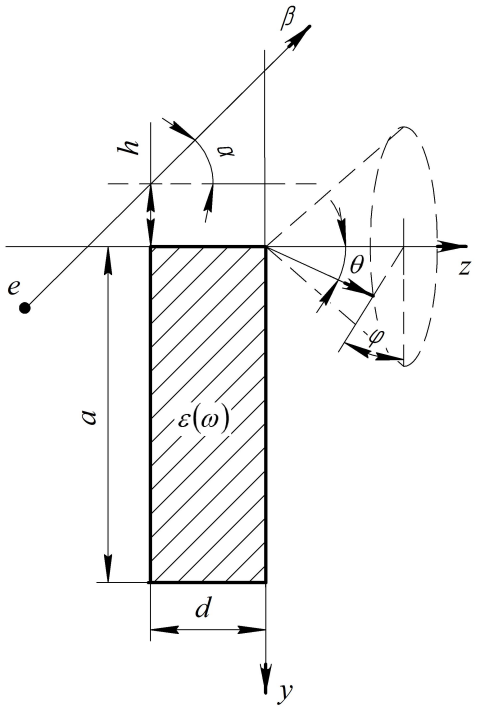

Figure 1. The calculation geometry.

Due to the fact that the polarization currents are induced in a finite volume determined by the target dimensions (see, for instance, Fig. 1), the solution of equation (3) can be found in the form:

$$\mathbf{H}^{pol}(\mathbf{r},\omega)=\frac{2\pi i}{c}\frac{\exp(ikr)}{r}\mathbf{k}\times\int_0^a dy'\int_{-d}^0\frac{\sigma(\omega)\mathbf{E}^0(k_x,y',z',\omega)}{\exp\left(i(k_y y'+k_z z')\right)}dz', \tag{4}$$

where $\mathbf{k}=\mathbf{e}\sqrt{\varepsilon}\omega/c$ is the wave vector, $\mathbf{e}=\mathbf{r}/\mathrm{r}$ is the unit vector along the photon emission. Taking into account the Snell's law of refraction the unit vector is

$$\mathbf{e}=\left\{\sin\theta_m\sin\varphi;\sin\theta_m\cos\varphi;\cos\theta_m\right\}=\frac{1}{\sqrt{\varepsilon}}\left\{\sin\theta\sin\varphi;\sin\theta\cos\varphi;\sqrt{\varepsilon-\sin^2\theta}\right\}. \tag{5}$$

Here θ_m and θ are the polar angles in the medium and in vacuum respectively, and φ is the azimuthal angle.

In (4) the integration is performed over the area confining the currents. In x direction, which is perpendicular to the plane of Fig. 1, we assume the screen is infinite. To solve the equation (4) we have to know the Fourier component of the charged particle field. Knowing a complete Fourier image of the field in the form [17–19]

$$\mathbf{E}^0(\mathbf{k},\omega) = \frac{4\pi i}{\omega}\frac{\mathbf{j}^0(\mathbf{k},\omega)(\omega/c)^2 - \mathbf{k}\Big(\mathbf{k}\mathbf{j}^0(\mathbf{k},\omega)\Big)}{\mathbf{k}^2 - (\omega/c)^2} \tag{6}$$

we can derive an expression for the Fourier component as

$$\mathbf{E}^0(k_x, y^{'}, z^{'}, \omega) = \int_{-\infty}^{+\infty} dk_y \int_{-\infty}^{+\infty} \mathbf{E}^0(\mathbf{k},\omega)\exp\Big(i(k_y y^{'} + k_z z^{'})\Big)dk_z. \tag{7}$$

In (6) the Fourier transform of the particle currents density is

$$\mathbf{j}^0(\mathbf{k},\omega) = \frac{e\mathbf{v}}{(2\pi)^3}\delta(\mathbf{k}\mathbf{v}-\omega)\exp(ik_y h), \tag{8}$$

where e is the particle charge, $\mathbf{v} = v\{0; -\sin\alpha; \cos\alpha\}$ is the particle velocity vector, $\delta(\mathbf{k}\mathbf{v}-\omega)$ is the Dirac delta-function, h is distance from the particles trajectory to the edge of the target.

Substituting equations (2) and (6)–(8) in (4) and integrating over the target volume we can derive an expression for the field strength of PR.

3. Dielectric properties of Carbon (C)

According to [22] the dielectric permittivity of a medium is defined by the following equation

$$\varepsilon(\omega) = 1 - \delta(\omega) + i\eta(\omega). \tag{9}$$

This equation is a function of radiation frequency. For metals and many other opaque materials in X-ray wavelength range the real part is smaller than unity. In this case generation of CR is impossible because the Cherenkov condition can not be fulfilled. However, in the vicinity of absorption edges the real part of (9) experiences a resonant rise reaching values above unity, therefore the Cherenkov condition might be fulfilled for relativistic particles. An example of

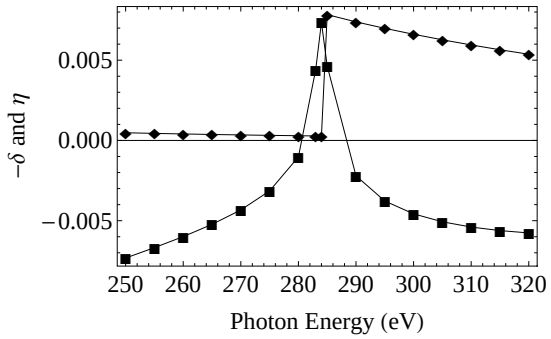

Figure 2. Dependence of the real $(-\delta)$ – ■ and imaginary (η) – ♦ parts of the dielectric constant of C in the vicinity of K-edge of absorption.

the such a rise in the vicinity of the K-edge of absorption of C is demonstrated in Fig. 2. The peak is rather sharp. One would expect the CR to be monochromatic. This phenomenon makes the CR attractive both for generating intense monochromatic X-ray radiation beams and its application for charged particle beam diagnostics.

4. Analysis of the radiation properties

In book [1] the authors demonstrated that in X-ray wavelength range when the particle moves in the vicinity of the target (diffraction Cherenkov radiation (CDR) geometry shown in Fig. 1) the CR has two maxima. Figure 3 illustrates the dependence of the PR intensity versus polar angle calculated for different incidence angles. The asymmetry appearing due to a small difference in the angle of incidence gives an opportunity to determine the angular jitter of the particle beam. In this geometry the calculation model is limited by the critical angle α_{cr}, i.e. the particle must not directly interact with the target. Its values will be determined by the following equation [19]:

$$\alpha_{cr} = \tan^{-1}\left(\frac{h}{d}\right). \tag{10}$$

If the particle actually crosses the screen (the geometry of transition Cherenkov radiation (CTR)) the model described by us in [20] can be used. In this case the asymmetry is smaller, but the CR intensity is higher than the TR intensity as it is shown in Fig. 3(b)). Moreover averaging over the beam angular divergence one may use the smoothing of the CTR peak as an indicator of the degree of the angular divergence.

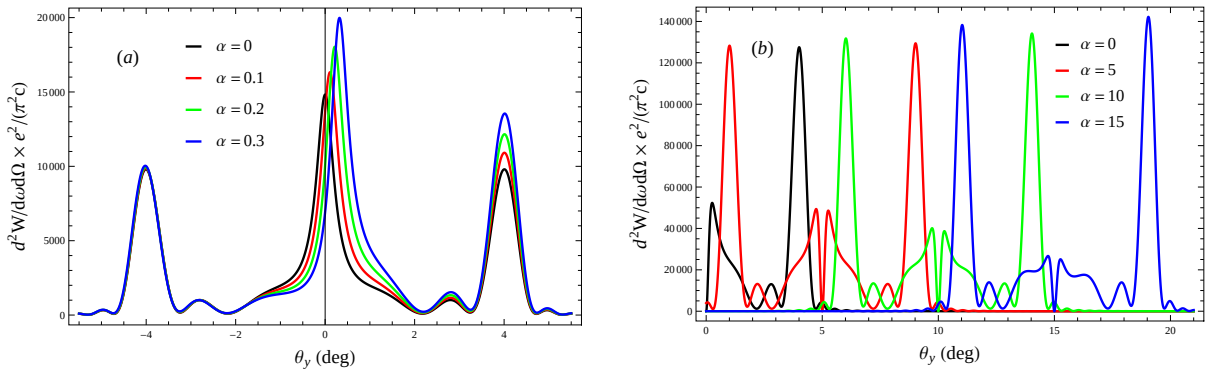

Figure 3. Dependence of the PR intensity on the projection observation angle $\theta_y = \theta\cos\varphi$ for different incidence angles α (degree): (a) for DR geometry; (b) for TR geometry. Parameters: $\gamma = 240$, $a = 70$ mm, $d = 5$ μm, $h = 0.1$ μm, $\hbar\omega = 284$ eV (K-edge of Carbon), $\varphi = 0, \pi$.

The photon yield can be optimized if we use the targets made of different materials. For example, Figure 4 presents dependences of the photon yield angular distributions calculated for Titanium ($\hbar\omega = 453.8$ eV), Silicon ($\hbar\omega = 99.8$ eV), and Aluminum ($\hbar\omega = 72.6$ eV) in the vicinity of L-edge of absorption. To show all these curves on a single plot the intensities were scaled accordingly. The scaling factors are shown on the graph in brackets. The Si targets (see Fig. 4(a)) are promising because even electrons with moderate relativistic energies are able to generate an easily detectable CR photon yield ($\sim 6\cdot 10^3$ ph/(el eV sr) in the distribution maximum). The use of CTR will lead to a significant increase of the intensity by 2–3 orders of magnitude (see Fig. 4(b)). The use of targets with large Z allows to significantly increase the CTR yield (compare, for example, the solid lines in Figs. 4(a) and 4(b)).

The X-ray CDR is very sensitive to the photon and electron energy. The latter property is the clearest in the electron energy range from keV to a few tens of MeV. The dependence on the photon energy is connected with the resonant behaviour of the dielectric permittivity in the vicinity of the absorption edges where the CR condition is fulfilled. Therefore the CDR spectrum represents a monochromatic line [14] with FWHM (Full Width at Half Maximum) of order of 1 – 1.5 eV. Figure 5(a) illustrates how strong the dependence on the photon energy is. Changing the photon energy by just a few eV the CR intensity goes from maximum to nothing

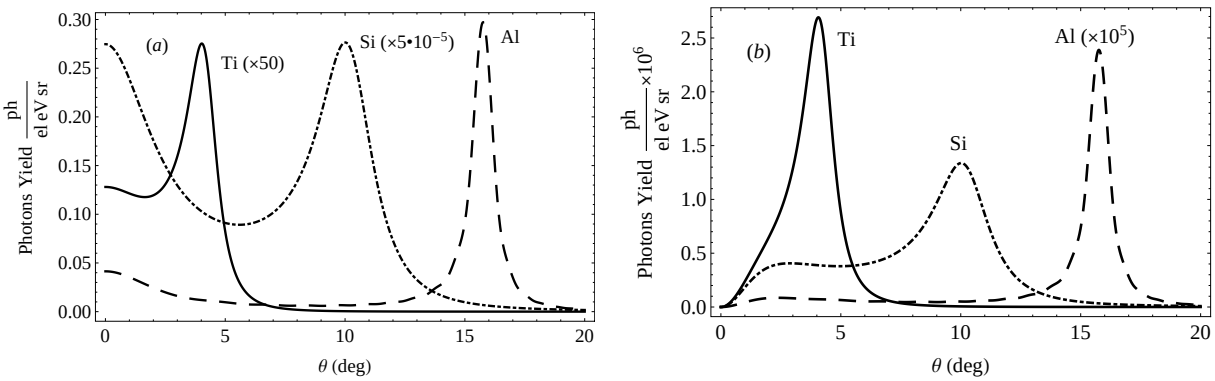

Figure 4. Dependence of the PR photons yield on the polar observation angle θ for different target materials: (a) for DR geometry; (b) for TR geometry. Parameters: $\gamma = 11$, $a = 70$ mm, $d = 5$ μm, $h = 0.1$ μm, $\varphi = \pi$.

whereas the DR peak remains. One may see a strong dependence of the position of the CDR peak in the angular distribution on the photon energy. For example, for given electron energy the change of the CDR photon energy on 1 eV leads to the peak shift on 1 degree.

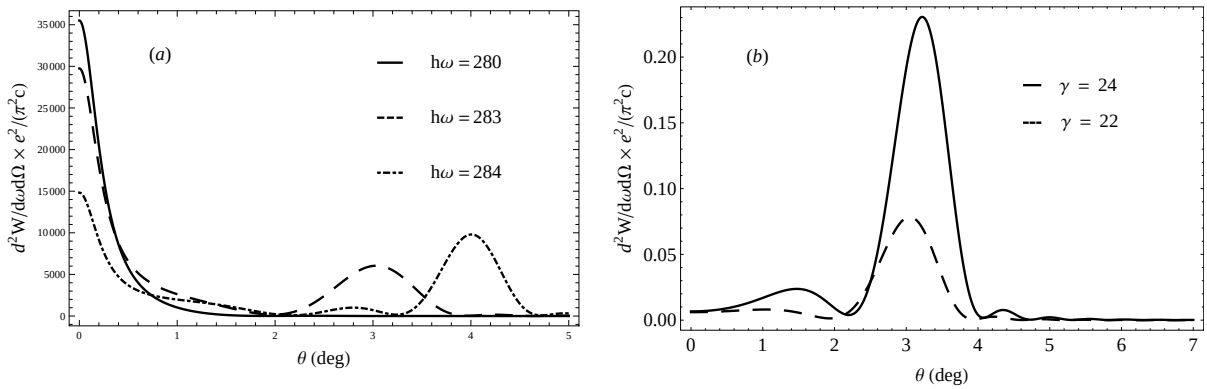

Figure 5. Dependence of the CDR intensity on the polar observation angle θ: (a) for different photon energies ($\gamma = 240$); (b) for different electron energies ($\hbar\omega = 284$ eV (K-edge of Carbon)). Parameters: $\alpha = 0$, $a = 70$ mm, $d = 5$ μm, $h = 0.1$ μm, $\varphi = \pi$.

In the range of moderately relativistic energies the CDR spectral-angular distribution allows to monitor the $< 10\%$ change in the electron energy (see, for instance, Fig. $5(b)$. Even a small change in the electron energy leads to a shift of the CDR peak position and intensity. With a larger change in the electron energy the shape of the distribution changes (compare, for example, dash-dotted line in Fig. $5(a)$ and solid line in Fig. $5(b)$). Nevertheless, for a energy resolution of 1% or less an experimental verification is necessary.

5. Conclusion

In this paper we have described the model for calculating PR characteristics in the X-ray range from a target of an arbitrary shape and arbitrary dielectric permittivity. For calculations we used a recently developed method of polarization currents. In the limiting cases of normal incidence the expressions obtained for the radiation intensity coincide with the results of papers [12–15] for TR geometry and book [1] for DR geometry.

We have demonstrated that CDR characteristics in X-ray region significantly depend on the energy of the emitted photons, because the CDR is only generated in the frequency region in the vicinity of the atomic absorption edges. This peculiarity can be explained by resonance behavior of the permittivity in the given frequency range. Due to strong non-linear dependence of the photon yield on the photon energy, the CR in the vicinity of the absorption edge is highly monochromatic. The CR photon yield is comparable, and for many cases significantly higher, then the TR and DR photon yields.

For the moderate relativistic energies $\gamma < 100$ the variation of the energy significantly influences the CDR characteristics. Such peculiarity can be used to measure the beam energy via the analysis of the spectral-angular distribution shape and intensity. In the vicinity of moderate relativistic energies one can increase the CDR intensity by increasing the angle of incidence. However, the spectral angular CDR density becomes very sensitive to the angle of the particle incidence with increasing the charged particle beam energy. Such peculiarity can be used to measure the particle beam angular jitter essentially for accelerator operation.

Summarizing the analysis and the peculiarities of the CDR in the vicinity of the absorption edges open a wide range of possibilities for charged particle beam diagnostics. Nevertheless, the model is still under analysis. A more detailed proposal devoted to the diagnostics will be presented later.

Acknowledgments

Authors are grateful to M V Shevelev for stimulating criticism and useful discussions. The work was partially supported by Russian Ministry of Science and Education within the grant No. 14.B37.21.0912 and the RFBR grants No. 14-02-31642-mol_a, No. 14-02-01032-A.

References

[1] Potylitsyn A P, Ryazanov M I, Strikhanov M N and Tishchenko A A 2010 *Diffraction Radiation from Relativistic Particles* (*Springer Tracts in Modern Physics* vol 239) (Berlin: Springer) p 278
[2] Karataev P, Aryshev A, Boogert S, Howell D, Terunuma N and Urakawa J 2011 *Phys. Rev. Lett.* **107** 174801
[3] Chiadroni E, Castellano M, Cianchi A, Honkavaara K, Kube G, Merlo V and Stella F 2011 *Phys. Rev.* ST–AB **14** 102803
[4] Blackmore V, Doucas G, Perry C, Ottewell B, Kimmitt M F, Woods M, Molloy S and Arnold R 2009 *Phys. Rev.* ST–AB **12** 032803
[5] Jin Z *et al* 2011 *Phys. Rev. Lett.* **107** 265003
[6] ILC Technical Design Report 2013 http://www.linearcollider.org/ILC
[7] XFEL Technical Design Report 2006 (*DESY*) 097 http://xfel.desy.de
[8] Loos H *et al* 2008 *Proc. FEL 08 (Gyeongju, South Korea)* p 485
[9] Sukhikh L G, Bajt S, Kube G, Popov Yu A, Potylitsyn A P and Lauth W 2012 *Proc. IPAC 12 (New Orleans, Louisiana, USA)* **MOPPR019** p 819
[10] Bobb L, Billing M, Chritin N, Karataev P and Lefevre T 2012 *Proc. IBIC 12 (Tsukuba, Japan)* **MOCC01** p 24
[11] Gogolev A, Potylitsyn A and Kube G 2012 *J. Phys: Conf. Ser.* **357** 012018
[12] Bazylev A V, Glebov V I, Denisov E I, Zhevago N K and Khlebnikov A S 1976 *JETP Lett.* **24** 371
[13] Bazylev A V, Glebov V I, Denisov E I, Zhevago N K, Kumakhov M A, Khlebnikov A S and Tsinoev V G 1981 *Sov. Phys. - JETP* **54** 884
[14] Knulst W, van der Wiel M J, Luiten O J and Verhoeven J 2003 *Appl. Phys. Lett.* **83** 4050
[15] Knulst W, van der Wiel M J, Luiten O J and Verhoeven J 2001 *Appl. Phys. Lett.* **79** 2999
[16] Moran M J, Chang B, Schneider M B and Maruyama X K 1990 *Nucl. Instrum. Methods* B **48** 287
[17] Karlovets D V and Potylitsyn A P 2009 *JETP Lett.* **90** 368
[18] Karlovets D V 2011 *Sov. Phys. - JETP* **113** 27
[19] Kruchinin K O and Karlovets D V 2012 *Russ. Phys. J.* **55** 9
[20] Konkov A S, Gogolev A S, Potylitsyn A P and Karataev P V 2013 *Proc. IBIC 13 (Oxford, UK)* **WEPF36** p 1
[21] Ginzburg V L and Tsytovich V N 1990 *Transition Radiation and Transition Scattering* (Bristol: A Hilger) p 433
[22] Henke B L, Gullikson E M and Davis J C 1993 *At. Data Nucl. Tables* **54** 181